
**DEFECTS AND IMPURITY CENTERS, DISLOCATIONS,
AND PHYSICS OF STRENGTH**

Kinetics of High-Temperature Precipitation in Dislocation-Free Silicon Single Crystals

V. I. Talanin* and I. E. Talanin

Classical Private University, ul. Zhukovskogo 70-b, Zaporozh'e, 69002 Ukraine

* e-mail: v.i.talanin@mail.ru

Received December 8, 2009; in final form, January 27, 2010

Abstract—The defect structure of dislocation-free silicon single crystals has been calculated using the approximate solution of the Fokker–Planck partial differential equations. It has been demonstrated that the precipitation starts to occur near the crystallization front due to the disappearance of excess intrinsic point defects on sinks whose role is played by oxygen and carbon impurities.

DOI: 10.1134/S1063783410100094

1. INTRODUCTION

At present, numerous studies of dislocation-free silicon single crystals have provided a wide variety of scientific data on the regularities of the formation and interaction of point defects and enormous practical experience has been gained in growing perfect single crystals. Such a large database on the structural properties and the influence of defects on the physico-chemical properties of silicon has not been created for other dislocation-free single crystals. At the same time, there has been no unified theoretical approach to the description of the interaction of point defects and the formation of an initial defect structure of dislocation-free silicon single crystals.

For example, electron microscopy investigations of quenched small-sized silicon single crystals grown by the crucibleless melting and Czochralski method, as well as large-sized silicon single crystals grown by the Czochralski method, have revealed that precipitates of impurities are the first to be formed and, only later, microvoids or interstitial dislocation loops arise [1–3]. At the same time, the model of dynamics of point defects has assumed that precipitation of an impurity occurs at the last stage of the formation of an initial defect structure during cooling of the as-grown crystal at temperatures below 1123 K [4–7]. Recent versions of this model have suggested that part of the vacancies (v) in the temperature range 1683–1373 K, due to the interaction with oxygen (O) and nitrogen (N) impurities, are bound into complexes of the vO , vO_2 , and vN types [8, 9]. After the formation of vacancy-type microvoids, the aforementioned complexes grow and take up vacancies. This model has ignored the growth of the complexes by means of the injection of intrinsic

interstitial silicon atoms and the interaction of an impurity with intrinsic interstitial silicon atoms [8, 9].

In order to perform a self-consistent treatment of the formation and growth of microdefects, it is necessary to meet conditions under which the corresponding model should include all the components involved in mass transfer in the system. In this regard, the purpose of the present work was to formulate and solve the problem of description of the process of precipitation during cooling of the crystal in the course of the growth in the high-temperature range.

2. MATHEMATICAL MODEL FOR THE FORMATION OF GROWN-IN MICRODEFECTS (PRECIPITATES)

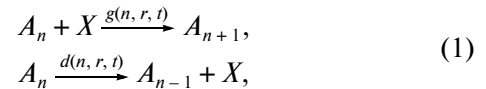
Let us consider a system of a growing undoped dislocation-free silicon single crystal. The concentrations of all point defects at the crystallization front are assumed to be equilibrium, and both the vacancies and the intrinsic interstitial silicon atoms are present in comparable concentrations [10]. During cooling of the crystal after passing through the diffusion zone, an excessive (nonequilibrium) concentration of intrinsic point defects appears. Excess intrinsic point defects disappear on sinks whose role in this process is played by uncontrollable (background) impurities of oxygen and carbon [2]. In real silicon crystals, the concentrations of carbon and oxygen impurities are higher than the concentrations of the intrinsic point defects. The formation of complexes between the intrinsic point defects and impurities is governed, on the one hand, by the fact that both the intrinsic point defects and the impurities are sources of internal stresses in the lattice (elastic interaction) and, on the other hand, by the Coulomb interaction between them (provided the

defects and the impurities are present in the charged state). The mathematical model under consideration allows for the elastic interaction and the absence of the recombination of intrinsic point defects in the high-temperature range [11]. The concentrations of intrinsic point defects $C_{i,v}(r, t)$ in the growing crystal satisfy the diffusion equation $\partial C_{i,v}/\partial t = D_{i,v}\Delta(C_{i,v} - C_{ie,ve})$, where r is the coordinate and t is the time. In the vicinity of the sinks (oxygen and carbon atoms), the concentration of intrinsic point defects $C_{ie,ve}$ is kept equilibrium, whereas the diffusion coefficients $D_{i,v}$ and the concentrations $C_{ie,ve}$ of intrinsic point defects decrease exponentially with decreasing temperature. Under these conditions, the formation of microvoids and interstitial dislocation loops is possible only at significant supersaturations of intrinsic point defects, which take place at a temperature $\sim T_{cr} = -300$ K (where T_{cr} is the crystallization temperature) [6].

Currently, the formation of precipitates in the high-temperature range $T \sim 1683\text{--}1403$ K has been calculated using the model of dissociative diffusion (migration of impurities) [12]. This approximation is valid at the initial stages of the formation of nuclei, when their sizes are small and the use of Fokker–Planck continuity differential equations is impossible. The calculations performed in the framework of this approximation have demonstrated that the edge of the reaction front of the formation of a complex (i.e., the “oxygen–vacancy” and “carbon–interstitial silicon atom” complex) is located at a distance of $\sim 3 \times 10^{-4}$ mm from the crystallization front [12]. This spacing represents a diffusion layer in which an excessive concentration of intrinsic point defects appears because the recombination of these defects at high temperatures is absent. The calculation of the defect structure of dislocation-free silicon single crystals at the stage of the formation and growth of oxygen and carbon precipitates in the model described in [12] agrees well with the experimental results available in the literature [1, 13]. This is true in regard to the temperatures of formation of grown-in microdefects; the experiments on quenching of the crystals; and the concentrations of $(I + V)$ -microdefects and $D(C)$ -microdefects, which were determined from the results of electron microscopy investigations ($\sim 10^{13}\text{--}10^{14}$ cm $^{-3}$) [2].

Now, we consider the modern approach based on solving systems of coupled discrete differential equations of quasi-chemical reactions for the description of the initial stages of the formation of nuclei of new phases and a similar system of Fokker–Planck continuity differential equations. The grown-in microdefects are treated as clusters of particles of different types, so that their formation and decay can be repre-

sented as a reaction involving random processes of attachment and detachment of particles X ,



where A_n is a cluster of the A type, which consists of n particles of the X type; $g(n, r, t)$ is the growth rate of the A_n cluster; and $d(n, r, t)$ is the decay rate of the A_n cluster. The concentration of the A_n clusters at the r point is determined by the function $f(n, r, t)$. The change of this function with time is described by the system of discrete kinetic differential equations

$$\begin{aligned} \frac{\partial f(n, r, t)}{\partial t} &= J(n, r, t) - J(n+1, r, t) \\ (n &= 2, 3, \dots, n_{\max}), \end{aligned} \quad (2)$$

$$\begin{aligned} J(n, r, t) &= g(n-1, r, t)f(n-1, r, t) \\ &\quad - d(n, r, t)f(n, r, t). \end{aligned}$$

The conservation of the number of X particles is described by the equation

$$\frac{\partial f(1, r, t)}{\partial t} = -J(2, r, t) - \sum_{n=2}^{n_{\max}} J(n, r, t), \quad (3)$$

where n_{\max} is the maximum number of X particles contained in the A cluster.

By expanding the gradually n -dependent functions g , d , and f into a Taylor series in terms to the second order included, the system of discrete equations is represented by the continuity partial differential equation (the Fokker–Planck equation) [14]

$$\frac{\partial f(n, r, t)}{\partial t} = -\frac{\partial I(n, r, t)}{\partial n}. \quad (4)$$

In this case, the flux of monomers in the space of n sizes is given by the formula

$$I(n, r, t) = Af - B\frac{\partial f}{\partial n} \quad (5)$$

and the kinetic coefficients A and B are described by the expressions

$$A = g - d - \frac{\partial B}{\partial n}, \quad B = \frac{g+d}{2}. \quad (6)$$

When solving the system of equations (2) and (4), the fluxes J and I are joined at the point $n = n_{\min}$. Then, the

law of conservation of the number of particles (3) is transformed into the form

$$\frac{\partial f(1, r, t)}{\partial t} = -J(2, r, t) - \sum_{n=2}^{n_{\min}-1} J(n, r, t) - \int_{n_{\min}}^{n_{\max}} I(n, r, t) dn. \quad (7)$$

Equation (4) represents a diffusion drift equation that describes the evolution of the distribution function f in the space of n sizes. The system of equations (2)–(7) makes it possible within a unified model to consider the processes of nucleation and the subsequent growth of the clusters [15]. The conventional boundary separating small and large clusters is considered to be $n = n_{\min}$, which, in the calculations, is assumed to fall in the range from 10 to 20. This quantity represents the boundary between the range of sizes ($n > n_{\min}$) in which the thermodynamic approach to the description of the physical processes can be considered valid and the range of sizes ($n < n_{\min}$) in which the atomic nature of these processes must be taken into account.

In order to describe the kinetics of the simultaneous nucleation and growth (dissolution) of a new phase particles of several types in a supersaturated solid solution of an impurity in silicon, it is necessary to consider a system consisting of oxygen and carbon atoms, vacancies, and intrinsic interstitial silicon atoms. The interaction in this system during cooling of the crystal from 1683 K results in the formation of oxygen and carbon precipitates [13]. In order to perform the computational experiments and to interpret their results, it is necessary to carry out a dimensional analysis of the kinetic equations and the conservation laws with the use of characteristic time constants and critical sizes of defects. This will make it possible to perform a comparative analysis of the joint evolution of oxygen and carbon precipitates and to optimize the computational algorithm for the numerical solution of the equations.

The nucleation and evolution of a complex system of grown-in microdefects (which consists of oxygen and carbon precipitates) during cooling of the crystal are described by the systems of coupled differential equations (2)–(7) for each type of defect. These systems are related by the laws of conservation of point defects, which determine the current values of their concentrations in the crystal and affect the rates of growth and dissolution of clusters of all types. For the case of a thin plane-parallel crystal plate of a large diameter, when the conditions in the plane parallel to the surface of the crystal can be considered to be uni-

form and the diffusion can be treated only along the normal to the surface (the z coordinate axis), the mass balance of point defects in the crystal is described by the system of diffusion equations for intrinsic interstitial silicon atoms, oxygen atoms, carbon atoms, and vacancies:

$$\begin{aligned} \frac{\partial C_O}{\partial t} &= D_O \frac{\partial^2 C_O}{\partial z^2} - \frac{\partial C_O^{\text{SiO}_2}}{\partial t}, \\ \frac{\partial C_C}{\partial t} &= D_C \frac{\partial^2 C_C}{\partial z^2} - \frac{\partial C_C^{\text{SiC}}}{\partial t}, \\ \frac{\partial C_i}{\partial t} &= D_i \frac{\partial^2 C_i}{\partial z^2} + \frac{\partial C_i^{\text{SiO}_2}}{\partial t} - \frac{\partial C_i^{\text{SiC}}}{\partial t}, \\ \frac{\partial C_v}{\partial t} &= D_v \frac{\partial^2 C_v}{\partial z^2} - \frac{\partial C_v^{\text{SiO}_2}}{\partial t} + \frac{\partial C_v^{\text{SiC}}}{\partial t}. \end{aligned} \quad (8)$$

In the system of equations (8), we took into account that the oxygen precipitates serves as sinks for oxygen atoms and vacancies and as sources of interstitial silicon atoms. Then, we can write the following equations:

$$\begin{aligned} C_O^{\text{SiO}_2} &= \sum_{n_O=2}^{n_O^{\min}-1} n_O f_{\text{SiO}_2}(n_O, z, t) \\ &+ \int_{n_O^{\min}}^{n_O^{\max}} n_O f_{\text{SiO}_2}(n_O, z, t) dn_O, \\ C_v^{\text{SiO}_2} &= \gamma_v C_O^{\text{SiO}_2}, \quad C_i^{\text{SiO}_2} = \gamma_i C_O^{\text{SiO}_2}. \end{aligned} \quad (9)$$

At the same time, the carbon precipitates, in turn, also serve as sinks for carbon atoms and interstitial silicon atoms and as sources for vacancies. Therefore, we can write

$$\begin{aligned} C_C^{\text{SiC}} &= \sum_{n_C=2}^{n_C^{\min}-1} n_C f_{\text{SiC}}(n_C, z, t) \\ &+ \int_{n_C^{\min}}^{n_C^{\max}} n_C f_{\text{SiC}}(n_C, z, t) dn_C, \\ C_v^{\text{SiC}} &= \gamma_v^* C_C^{\text{SiC}}, \quad C_i^{\text{SiC}} = \gamma_i^* C_C^{\text{SiC}}. \end{aligned} \quad (10)$$

In the general case, the proportionality factors γ_v , γ_i , γ_v^* , and γ_i^* can depend on the quantities n_O and n_C and are determined by the conditions of thermodynamic equilibrium [16, 17]. Moreover, in the system of equations (8), the recombination of pairs of intrinsic interstitial silicon atoms and vacancies is ignored [2].

The corresponding system of coupled Fokker–Planck equations can be transformed into the dimensionless form

$$\begin{aligned}\frac{\partial \tilde{f}_{\text{SiO}_2}}{\partial \tau} &= -\frac{\partial I_{\text{SiO}_2}}{\partial \tilde{v}_O}, \\ \frac{\partial \tilde{f}_{\text{SiC}}}{\partial \tau} &= -\frac{t_0}{t_C} \frac{\partial I_{\text{SiC}}}{\partial \tilde{v}_C},\end{aligned}\quad (11)$$

where $\tau = \frac{t}{t_0}$ is the dimensionless time. The time constants in the system of equations (11) are given by the expressions $t_0 = (n_0^{\text{cr},0})^2 / g_{\text{SiO}_2}^0$ and $t_C = (n_C^{\text{cr},0})^2 / g_{\text{SiC}}^0$, where the critical growth rates of the precipitates are defined as $g_{\text{SiO}_2}^0 = N_0^0 v_O \exp(-G_{\text{act}}^{\text{SiO}_2} / kT)$ and $g_{\text{SiC}}^0 = N_C^0 v_C \exp(-G_{\text{act}}^{\text{SiC}} / kT)$. The normalized sizes of the precipitates are determined in the system of equations (11) as follows: $\tilde{v}_O = n_O / n_0^{\text{cr},0}$ and $\tilde{v}_C = n_C / n_C^{\text{cr},0}$, where n_0^{cr} and n_C^{cr} are the normalizing critical sizes of the precipitates. The quantities $N_0^0 = 4\pi(r_0^{\text{cr},0})^2 \delta_{\text{SiO}_2} C_O^{\text{eq}}$ and $N_C^0 = 4\pi(r_C^{\text{cr},0})^2 \delta_{\text{SiC}} C_C^{\text{eq}}$ are the numbers of particles in the vicinity of the corresponding precipitates with critical sizes. The size distribution functions of the precipitates in the system of equations (11) are normalized to the initial concentrations of the corresponding nucleation centers:

$$\tilde{f}_{\text{SiO}_2} = \frac{f_{\text{SiO}_2}}{f_{\text{SiO}_2}^0}, \quad \tilde{f}_{\text{SiC}} = \frac{f_{\text{SiC}}}{f_{\text{SiC}}^0}. \quad (12)$$

The fluxes of particles on the right-hand sides of the system of equations (11) are described by the expressions

$$\begin{aligned}A_{\text{SiO}_2} &= (\tilde{g}_{\text{SiO}_2} - \tilde{d}_{\text{SiO}_2}) n_0^{\text{cr},0} - \frac{\partial B_{\text{SiO}_2}}{\partial \tilde{v}_O}, \\ A_{\text{SiC}} &= (\tilde{g}_{\text{SiC}} - \tilde{d}_{\text{SiC}}) n_C^{\text{cr},0} - \frac{\partial B_{\text{SiC}}}{\partial \tilde{v}_C},\end{aligned}\quad (13)$$

in which the following notation is used for the normalized kinetic coefficients:

$$A_{\text{SiO}_2} = (\tilde{g}_{\text{SiO}_2} - \tilde{d}_{\text{SiO}_2}) n_0^{\text{cr},0} - \frac{\partial B_{\text{SiO}_2}}{\partial \tilde{v}_O}, \quad (14)$$

$$\begin{aligned}A_{\text{SiC}} &= (\tilde{g}_{\text{SiC}} - \tilde{d}_{\text{SiC}}) n_C^{\text{cr},0} - \frac{\partial B_{\text{SiC}}}{\partial \tilde{v}_C}, \\ B_{\text{SiO}_2} &= \frac{\tilde{g}_{\text{SiO}_2} + \tilde{d}_{\text{SiO}_2}}{2}, \quad B_{\text{SiC}} = \frac{\tilde{g}_{\text{SiC}} + \tilde{d}_{\text{SiC}}}{2}.\end{aligned}\quad (15)$$

The normalized rates of growth and dissolution of the precipitates in expressions (14) and (15) take the form

$$\begin{aligned}\tilde{g}_{\text{SiO}_2} &= \frac{g_{\text{SiO}_2}}{g_{\text{SiO}_2}^0}, \quad \tilde{g}_{\text{SiC}} = \frac{g_{\text{SiC}}}{g_{\text{SiC}}^0}, \\ \tilde{d}_{\text{SiO}_2} &= \frac{d_{\text{SiO}_2}}{g_{\text{SiO}_2}^0}, \quad \tilde{d}_{\text{SiC}} = \frac{d_{\text{SiC}}}{g_{\text{SiC}}^0}.\end{aligned}\quad (16)$$

The critical size of the precipitates can be determined according to [17] from the expressions

$$r_0^{\text{cr}} = \frac{2\sigma u V_p}{kT \ln(S_O S_i^{-\gamma_i} S_v^{-\gamma_v}) - 6\mu\delta\epsilon u V_p}, \quad (17)$$

$$r_C^{\text{cr}} = \frac{2\sigma u V_p}{kT \ln(S_C S_i^{\gamma_i} S_v^{-\gamma_v}) - 6\mu\delta\epsilon u V_p}, \quad (18)$$

where $S_O = C_O / C_{C_O}^{\text{eg}}$, $S_C = C_C / C_C^{\text{eg}}$, $S_i = C_i / C_i^{\text{eg}}$, and $S_v = C_v / C_v^{\text{eg}}$ are the supersaturations of the oxygen atoms, carbon atoms, intrinsic interstitial silicon atoms, and vacancies, respectively; σ is the density of the surface energy of the interface between the precipitate and the matrix; μ is the shear modulus of silicon; δ and ϵ are the relative linear and volume misfit strains of the precipitate and the matrix, respectively; γ_i and γ_v are the fractions of the intrinsic interstitial silicon atoms and vacancies per impurity atom attached to the precipitate, respectively; V_p is the molecular volume of the precipitate; and $u = (1 + \gamma_i x + \gamma_v x)^{-1} \left(\frac{1 + \epsilon}{1 + \delta} \right)^3$.

The number of impurity atoms in the compressed precipitates with the radii r_0 and r_C is determined according to [18, 19] from the formula

$$n_{O,C} = \frac{4\pi r_{O,C}^3 (1 + \gamma_i x + \gamma_v x) \left(\frac{1 + \delta}{1 + \epsilon} \right)^3}{3V_p}, \quad (19)$$

where V_p is the volume of the precipitate; x is the fraction of impurity atoms per intrinsic defect, $x \leq 2$; $\gamma_i \leq 1/2$; and $\gamma_v \leq 1/2$.

3. RESULTS AND DISCUSSION

The calculations were performed using the following data: $V_p = 4.302 \times 10^{-2}$ (SiO₂) and 2.04×10^{-2} nm³ (SiC); $\sigma = 310$ (SiO₂) and 1000 erg/cm² (SiC); $\mu = 6.41 \times 10^{10}$ Pa; $\delta = 0.3$; $\epsilon = 0.15$ [15]; $\gamma_i = 0.4$; $\gamma_v = 0.1$; $x = 1.5$; $\delta_{\text{SiO}_2} = 0.5431$ nm; $\delta_{\text{SiC}} = 0.4359$ nm; $C_O^{\text{eq}} = 8 \times 10^{16}$ cm⁻³; $C_C^{\text{eq}} = 1 \times 10^{16}$ cm⁻³; $D_O = 0.17 \exp(-2.54 \text{ eV}/kT)$; $D_C = 1.9 \exp(-3.1 \text{ eV}/kT)$;

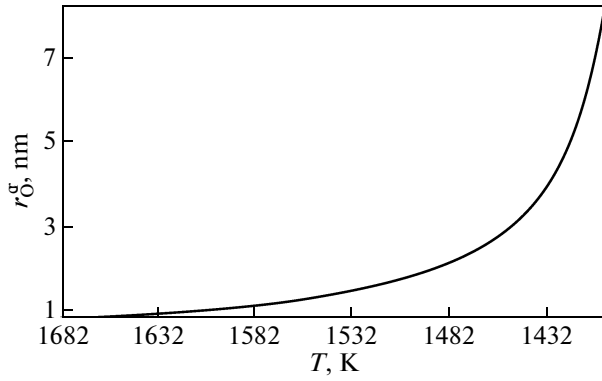


Fig. 1. Temperature dependence of the critical radius of the oxygen precipitate during cooling of the as-grown crystal.

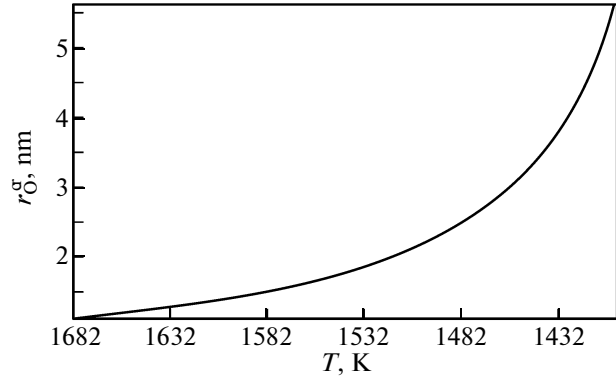


Fig. 2. Temperature dependence of the critical radius of the carbon precipitate during cooling of the as-grown crystal.

$G_{\text{act}}^{\text{SiO}_2} = 2.54 \text{ eV}$; $G_{\text{act}}^{\text{SiC}} = 3.17 \text{ eV}$; and $k = 8.6153 \times 10^{-5} \text{ eV/K}$.

When analyzing the evolution of grown-in microdefects during cooling of the crystal in the course of its growth, the important parameters are the characteristic constants in the size space: the critical sizes of the corresponding grown-in microdefects and the related characteristic time constants, which specify the scale of changes in the size distribution function of microdefects with time. The time constants in the system of equations (11) allow one to calculate the normalizing sizes $n_{\text{O}}^{\text{cr},0}$ and $n_{\text{C}}^{\text{cr},0}$; for this purpose, the supersaturations corresponding to the complete inclusion of the oxygen and carbon atoms in the precipitates are substituted into expressions (17) and (18). In each of these expressions, the supersaturations of the remaining point defects are assumed to be equal to unity.

An increase in the supersaturations of point defects (oxygen and carbon atoms, intrinsic interstitial silicon atoms, and vacancies) leads to a decrease in the corresponding critical size of the precipitates and favors an acceleration of their growth. A decrease in the characteristic times also leads to an acceleration of the precipitation with an increase in the supersaturations of the point defects. The opposite trend is observed when the crystal is cooled from the crystallization temperature.

An important property of the characteristic times is their inverse proportionality to the products of the characteristics of point defects (diffusion coefficients and equilibrium concentrations):

$$t_{\text{O}} \sim (D_{\text{O}}C_{\text{O}}^{\text{eq}})^{-1}, \quad t_{\text{C}} \sim (D_{\text{C}}C_{\text{C}}^{\text{eq}})^{-1}. \quad (20)$$

Since the product of the characteristics of point defects for oxygen atoms considerably exceeds the analogous product for carbon atoms, the rate of evolution of the size distribution function of the carbon pre-

cipitates should exceed the corresponding rate for oxygen precipitates. This means that the evolution of the microdefect structure of dislocation-free silicon single crystal during cooling of the as-grown crystal is determined predominantly by the growth rate of the oxygen precipitates. A detailed quantitative information on the characteristics of the primary grown-in microdefects can be obtained by numerically calculating the system of equations (11).

The algorithm used for solving the problem of simulation of the simultaneous growth and dissolution of the oxygen and carbon precipitates due to the interaction of point defects during cooling of the crystal from the crystallization temperature is based on the monotonic explicit difference scheme of the first-order accuracy as applied to the Fokker–Planck equations (11).

Figures 1 and 2 show the temperature dependences of the critical radii of the oxygen and carbon precipitates, respectively. Near the crystallization front (at the temperature $T = 1682 \text{ K}$), the critical nucleus size of the oxygen precipitate is equal to 0.81 nm and the critical nucleus size of the carbon precipitate is approximately 1.1 nm . The minimum values of $n_{\text{O}}^{\text{cr}} = n_{\text{O}}^{\text{cr},0}$ and $n_{\text{C}}^{\text{cr}} = n_{\text{C}}^{\text{cr},0}$ are reached in the initial state at the temperature $T = 1682 \text{ K}$ and increase with decreasing temperature. An increase in the critical radius of the precipitates during cooling leads to an abrupt decrease in their growth rate and, accordingly, to an abrupt decrease in the precipitation rate.

The simulation of the kinetics of defect formation during cooling of the growing crystal according to an exponential law in the temperature range from 1682 to 1403 K is shown in Figs. 3 and 4. In the presented computational experiment, it was assumed that the concentrations of nucleation centers for the oxygen and carbon precipitates are approximately equal to 10^{12} cm^{-3} . These values correspond to the experimen-

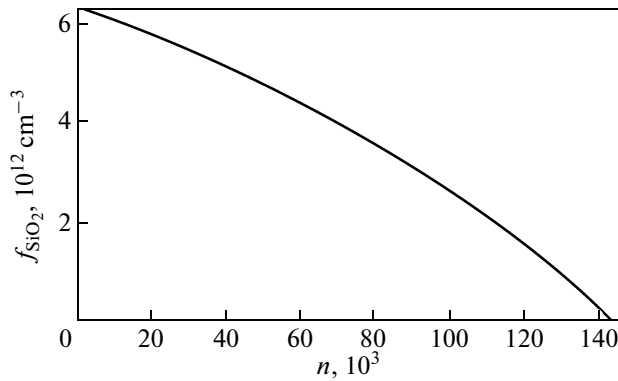


Fig. 3. Size distribution function of oxygen precipitates $f_{\text{SiO}_2}(n)$ during cooling of the as-grown crystal.

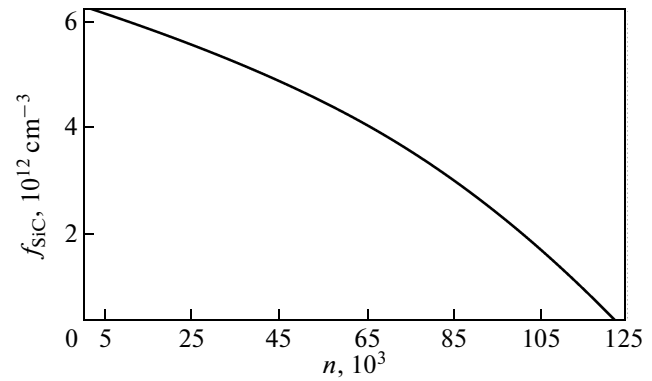


Fig. 4. Size distribution function of carbon precipitates $f_{\text{SiC}}(n)$ during cooling of the as-grown crystal.

tal data obtained from transmission electron microscopy [2]. The size distribution functions of the oxygen and carbon spherical precipitates are presented in Figs. 3 and 4, respectively.

These functions demonstrate that intrinsic point defects (vacancies and intrinsic interstitial silicon atoms) exert a significant influence on the dynamics of mass exchange and mass transfer of point defects between the oxygen and carbon precipitates. The absorption of vacancies by the growing oxygen precipitates leads to the emission of silicon atoms into interstitial positions. The intrinsic interstitial silicon atoms, in turn, interact with the growing carbon precipitates, which, in the process of growth, supply vacancies for growing oxygen precipitates. This interaction leads to such a situation that, first, the growth of the precipitates is suppressed more weakly because of the slower increase in the supersaturation of the intrinsic point defects in the bulk of the growing crystal and, second, the critical radius of the formation of carbon precipitates increases more slowly, which favors a more rapid growth of the carbon precipitates.

The higher rate of the evolution of the size distribution function for carbon precipitates can be associated with the higher mobility of interstitial silicon atoms as compared to vacancies in the high-temperature range. It can be assumed that the mutual formation and growth of oxygen and carbon precipitates result in a lower rate of the evolution of the size distribution function of the oxygen precipitates, regardless of their smaller critical size at the initial instant of time, owing to the effect of the carbon impurity.

The computational experiment carried out in this work is confirmed by the experimental results reported by Ueki et al. [20]. These authors used low-energy electron spectroscopy and Auger electron spectroscopy and demonstrated that the forming carbon precipitates hinder growth of oxygen precipitates and

simultaneously bring about the formation of new oxygen precipitates. Similar results were obtained by Itsumi et al. [21] and Yamanaka [22], who used transmission electron microscopy and established that oxygen and carbon precipitates are formed during cooling of a 150-mm-diameter crystal, which grows under the conditions $V/G > \xi_{\text{crit}}$ in the temperature range from 1682 to 1403 K. These precipitates are precursors and nucleation centers for vacancy microvoids formed during cooling of the crystal below 1403 K [3, 23, 24]. In this regard, we should note the study by Albrecht et al. [25], who also used transmission electron microscopy and proved the formation of platelike and amorphous carbon precipitates in the $\{111\}$ and $\{100\}$ crystal planes.

The analysis of the theoretically calculated curves has demonstrated their good agreement with the experimental data. This is true in regard to the temperatures of formation of primary grown-in microdefects; the experiments on quenching of crystals; and the concentrations of $(I + V)$ -microdefects and $D(C)$ -microdefects, which were determined from the results of transmission electron microscopy investigations ($\sim 10^{13} \text{ cm}^{-3}$) [2].

The results of approximate calculations of the Fokker–Planck partial differential equations correlate well with the results of the analytical solution of the equations in the consistent model of dissociative diffusion in the approximation of strong complex formation [12]. The main advantage of these two models is that they complement each other. In particular, the critical size distribution functions of the oxygen and carbon precipitates can be found only from the Fokker–Planck continuity differential equations, whereas the consistent model of dissociative diffusion in the approximation of strong complex formation has failed to obtain these functions. At the same time, the model of dissociative diffusion makes it possible to analyze

the processes occurring in the diffusion region near the crystallization front. Of special note is the fact that these mathematical models, together with the experimental results obtained from the investigation of quenched crystals, have demonstrated that the nucleation processes occur very rapidly near the crystallization front.

4. CONCLUSIONS

It should be noted that the processes of formation and growth of precipitates during cooling of the crystal is a controlling stage in the formation of the grown-in defect structure of dislocation-free silicon single crystals. At this stage, the formation and growth of oxygen and carbon precipitates occur in the temperature range from 1682 to 1403 K.

The defect structure of dislocation-free silicon single crystals at the stage of the nucleation and growth of oxygen and carbon precipitates has been calculated using the approximate solution of the Fokker–Planck partial differential equations. It has been demonstrated that the precipitation starts to occur near the crystallization front due to the disappearance of excess intrinsic point defects on sinks whose role is played by oxygen and carbon impurities.

REFERENCES

1. V. I. Talanin, *Simulation of the Defect Structure of Dislocation-Free Silicon Single Crystals and Their Properties* (ZIGMU, Zaporozh'e, Ukraine, 2007) [in Russian].
2. V. I. Talanin and I. E. Talanin, in *New Research on Semiconductors*, Ed. by T. B. Elliot (Nova Science, New York, United States, 2006), p. 31.
3. M. Itsumi, *J. Cryst. Growth* **237–239**, 1773 (2002).
4. V. V. Voronkov, *J. Cryst. Growth* **59**, 625 (1982).
5. T. Sinno and R. A. Brown, *J. Electrochem. Soc.* **146**, 2300 (1999).
6. M. S. Kulkarni, V. V. Voronkov, and R. Falster, *J. Electrochem. Soc.* **151**, G663 (2004).
7. A. I. Prostomolotov and N. A. Verezub, *Solid State Phenom.* **131–133**, 283 (2008).
8. M. S. Kulkarni, *J. Cryst. Growth* **303**, 438 (2007).
9. M. S. Kulkarni, *J. Cryst. Growth* **310**, 324 (2008).
10. M. Akatsuka, M. Okui, S. Umeno, and K. Sueoka, *J. Electrochem. Soc.* **150**, G587 (2003).
11. V. I. Talanin and I. E. Talanin, *Fiz. Tverd. Tela (St. Petersburg)* **49** (3), 450 (2007) [*Phys. Solid State* **49** (3), 467 (2007)].
12. V. I. Talanin, I. E. Talanin, and V. V. Voronin, *Can. J. Phys.* **85**, 1459 (2007).
13. V. I. Talanin, *Izv. Vyssh. Uchebn. Zaved., Mater. Élektron. Tekh.*, No. 4, 27 (2007).
14. S. Senkader, J. Esfandyari, and G. Hobler, *J. Appl. Phys.* **78**, 6469 (1995).
15. M. M. Belova, M. N. Moskal'kov, A. E. Rudich, S. I. Olikhovskii, and E. V. Kochelab, *Metallofiz. Novejšie Tekhnol.* **29**, 427 (2007).
16. V. V. Voronkov and R. Falster, *J. Appl. Phys.* **86**, 2100 (1999).
17. J. Vanhellmont, *J. Appl. Phys.* **78**, 4297 (1995).
18. J. Vanhellmont and C. Claeys, *J. Appl. Phys.* **62**, 3960 (1987).
19. V. V. Voronkov and R. Falster, *J. Appl. Phys.* **91**, 5802 (2002).
20. T. Ueki, M. Itsumi, and T. Takeda, *Jpn. J. Appl. Phys.* **38**, 5695 (1999).
21. M. Itsumi, M. Maeda, S. Ohfuji, and T. Ueki, *Jpn. J. Appl. Phys.* **38**, 5720 (1999).
22. H. Yamanaka, *Jpn. J. Appl. Phys.* **33**, 3319 (1994).
23. Y. Yanase, H. Nishihata, T. Ochiai, and H. Tsuya, *Jpn. J. Appl. Phys.* **37**, 1 (1998).
24. T. Ueki, M. Itsumi, T. Takeda, K. Yoshida, A. Takaoka, and S. Nakajima, *Jpn. J. Appl. Phys.* **37**, L771 (1998).
25. M. Albrecht, S. B. Aldabergenova, Sh. B. Baiganatova, G. Frank, T. I. Taurbaev, S. Christiansen, and H. P. Strunk, *Cryst. Res. Technol.* **35**, 899 (2000).

Translated by N. Pomortseva